

Measurement of the rate coefficient for the reaction of O(¹D) with H₂O and re-evaluation of the atmospheric OH production rate

Edward J. Dunlea and A. R. Ravishankara

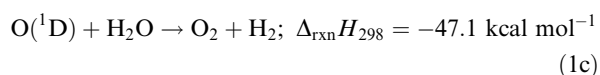
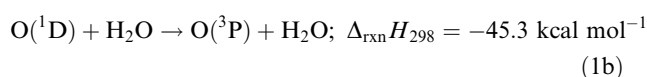
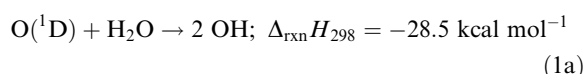
Aeronomy Laboratory, National Oceanic and Atmospheric Administration, 325 Broadway, Boulder, CO 80305, USA and Department of Chemistry and Biochemistry, The Cooperative Institute for Research in Environmental Sciences, University of Colorado, Boulder, CO 80309, USA. E-mail: dunlea@post.harvard.edu and ravi@alnoaa.gov; Fax: 303-497-5822; Tel: 303-497-5821

Received 18th February 2004, Accepted 29th March 2004
First published as an Advance Article on the web 7th May 2004

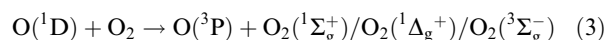
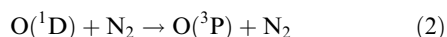
The rate coefficient for the reaction of O(¹D) with H₂O (Reaction 1), whose value is critical for calculating production rates of the OH radical in the atmosphere, was measured over a range of atmospherically relevant temperatures. The temporal profile of O(³P) following photolytic production of O(¹D) in the presence of water vapor was used to determine a temperature dependent value for k_1 of $(1.45 \pm 0.34) \times 10^{-10} \exp((89 \pm 65)/T)$ cm³ molecule⁻¹ s⁻¹, where the quoted errors are at the 95% confidence level, include estimated systematic errors and $\sigma_A = A \sigma_{\ln A}$. In addition, ratios of rate coefficients for quenching of O(¹D) by N₂ and O₂ (k_2 and k_3) to that for Reaction 1 were determined to be $k_2/k_1 = (0.13 \pm 0.04)$ and $k_3/k_1 = (0.19 \pm 0.09)$ by measuring the relative OH concentration produced from Reaction 1 in the presence of various concentrations of N₂ or O₂. Combining our results of this work with previous measurements of k_1 , we recommend a value for $k_1 = (1.62 \pm 0.27) \times 10^{-10} \exp((65 \pm 50)/T)$ cm³ molecule⁻¹ s⁻¹, where the quoted errors are 95% confidence level, include estimated systematic errors and $\sigma_A = A \sigma_{\ln A}$. Based on these results, the uncertainty in the calculated atmospheric OH production rate due to the uncertainty in these rate coefficients is reduced from $\pm 50\%$ to $\pm 20\%$.

Introduction

The hydroxyl radical (OH) plays a critical role in the chemistry of the atmosphere (see ref. 1 for example). The major source of OH in the troposphere and stratosphere is the photolysis of ozone (O₃) producing oxygen atoms in the first electronically excited state (O(¹D)), followed by the reaction of O(¹D) with water vapor (H₂O):



Reaction channel (1a) is known to be the dominant channel for atmospheric conditions.² At all altitudes, this reaction competes with the quenching of O(¹D) to its ground state, O(³P), by other atmospheric gases, primarily N₂ and O₂:



Thus the rate of OH production is given by:

$$\frac{d[\text{OH}]}{dt} = J_{\text{O}^1\text{D}} \times [\text{O}_3] \times \frac{k_1[\text{H}_2\text{O}]}{k_1[\text{H}_2\text{O}] + k_2[\text{N}_2] + k_3[\text{O}_2]} \quad (I)$$

where $J_{\text{O}^1\text{D}}$ is the first order rate coefficient for photolysis of O₃ that yields O(¹D). Currently recommended values² of the rate coefficients for Reactions (1)–(3), k_1 – k_3 , have uncertainties of $\pm 40\%$ or more (corresponding to approximately two standard deviations; all uncertainties in this paper are reported at this

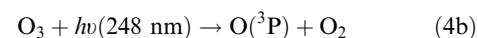
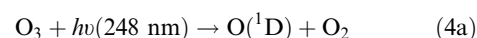
2σ , or 95% confidence, level for consistency). These uncertainties compound into an overall uncertainty in the OH production rate as large as $\pm 50\%$, depending on the altitude, due to uncertainties in rate coefficients alone. When uncertainties in the atmospheric concentrations of the involved gases are included, the calculated OH production rate is even more uncertain. Recent studies from our laboratory and others have decreased the uncertainties in the values of k_2 and k_3 .^{3–6} We focus on k_1 in this study.

This study involved two complimentary parts to improve upon the accuracy of the calculated OH production rate. First, we measured absolute values of the rate coefficients for Reaction (1) over the temperature range 235 to 370 K *via* pulsed laser photolytic creation of O(¹D) followed by resonance fluorescence detection of O(³P). Second, we measured k_1 relative to k_2 and k_3 using pulsed laser photolysis to create O(¹D) and pulsed laser induced fluorescence to detect OH generated by the reaction of O(¹D) with H₂O. Lastly, we used a simple box model to characterize the implications of our measured rate coefficients on the calculated atmospheric OH production rate.

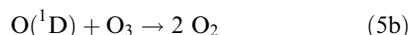
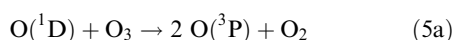
Experiments

Absolute rate coefficient measurement

The apparatus and experimental procedures used in the present study have been described previously.^{7–9} Therefore, only the details essential for describing this study are given here. O(¹D) was generated by photolyzing O₃ with a 248 nm excimer laser (KrF; repetition rate ~ 4 Hz),



$O(^3P)$ was produced from $O(^1D)$ via its reaction with O_3 :



and via quenching by the helium carrier gas (and associated impurities). A microwave discharge lamp ran as a continuous VUV light source to excite $O(^3P)$ near 131 nm. A solar blind photomultiplier tube, whose output was fed to a multichannel scaler through an amplifier discriminator, detected resonant fluorescence from the excited oxygen atoms. The entire temporal profile of $O(^3P)$ was obtained for each laser shot. Hundreds to thousands of temporal profiles were added together to produce an $O(^3P)$ temporal profile with excellent signal-to-noise ratio; this profile was fit to an analytical expression to derive the first order rate coefficient for the removal of $O(^1D)$.⁶ Various amounts of H_2O were added, while keeping the O_3 concentration and pressure constant, to determine the overall rate coefficient for $O(^1D)$ removal by H_2O , k_1 . The uncertainty in the measured value of k_1 is due mainly to the uncertainty in water vapor concentration. Therefore, a great deal of effort was spent on quantifying $[H_2O]$, which is described in the section on water vapor concentration measurements.

Relative rate coefficient measurements

The PP-LIF technique for the measurement of OH has been used extensively in our laboratory^{10–12} to measure rate coefficients and quantum yields. We created a pulse of $O(^1D)$ and/or OH radicals via 248 nm excimer laser photolysis of either ozone or H_2O_2 and detected OH via pulsed laser induced fluorescence. We excited the $Q_1(1)$ line of the OH ($A^2\Sigma(v=1) \leftarrow X^2\Pi(v=0)$) transition at 281.9 nm and detected fluorescence around 308 nm with a photomultiplier tube (PMT) equipped with a band-pass filter centered at 308 nm and oriented orthogonal to both photolysis and probe laser beams. The signal from the PMT was fed into a gated charge integrator and the signals due to 10 pulses were averaged by a computer for 100 laser pulses. The signal-to-noise ratio, defined as the signal above the background divided by one standard deviation of the background, was 1 for 1.3×10^8 molecule cm^{-3} in 50 Torr N_2 .

Fig. 1 shows how all gases were mixed prior to entering the reactor. Calibrated flow meters were used to measure flow rates of N_2 , O_2 , and He carrier gas. Concentrations of N_2 and O_2 were determined from the mass flow rates and the pressure in the reactor; the uncertainty in their concentrations is estimated to be $\pm 8\%$ (95% confidence level).³ A stable flow of water vapor was produced by bubbling a small flow of UHP He through a liquid sample of distilled H_2O and the concentration of H_2O in the gas mixture was measured via absorption of 185 nm light in a 10 cm long glass cell

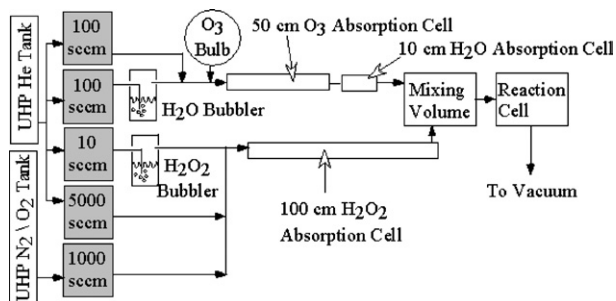


Fig. 1 Schematic showing the set up of the gas flows used with the LIF experiments to measure the yield of OH in the photolysis of a mixture of O_3 , H_2O , H_2O_2 , He and N_2 or O_2 . Mass flow meters are shown in grey.

(see following section). To introduce the small concentrations of O_3 necessary in these experiments, we used very small flow rates (~ 1 sccm) of a dilute ($\sim 1\%$) mixture of O_3 in He. The O_3 concentration was measured *in situ* via absorption at 253.7 nm in a 50 cm long glass cell and diluted by a measured flow of He. As with H_2O , H_2O_2 was delivered via a small flow of UHP He bubbled through a liquid sample of concentrated H_2O_2 . The H_2O_2 concentration was measured via absorption at 213.9 nm (Zn lamp) in a 100 cm cell. Based on the uncertainties in the absorption cross sections and measured signals, the uncertainties in the concentrations of the O_3 and H_2O_2 in the reactor were each estimated to be $\pm 5\%$ (95% confidence level).

For the relative rate coefficient measurements described below, the flow rates of He and of N_2 or O_2 were varied such that the total flow rate through the reactor was constant. The flow rates of H_2O , O_3 , and H_2O_2 were kept constant. This approach maintained approximately the same pressure and concentrations of H_2O , H_2O_2 , and O_3 , while allowing variations in the N_2 or O_2 concentrations.

Water vapor concentration measurement

Accurately determining the concentration of water vapor can be difficult because it may stick to the walls or desorb from the walls. Therefore, we directly measured H_2O concentration in the gas flow entering or leaving the reactor. To maintain a small but stable flow of water vapor, we bubbled a small flow (0 to 100 sccm) of He gas through distilled liquid H_2O maintained at 273 K (by immersing the bubbler in an ice/water bath) and then metered out a small flow through a needle valve before mixing it with rest of the carrier gas flow. We could achieve a stable flow of water vapor within a few minutes and it typically remained constant for at least 15 min, the time required to measure a good temporal profile of $O(^3P)$ or OH.

Water vapor concentrations were determined via absorption of Lyman- α radiation (121.6 nm) for measuring k_1 . For the relative rate coefficient measurements, water vapor concentrations were measured via absorption at 184.9 nm. In separate experiments, these two methods were intercompared. In addition, they were compared with water vapor concentration that was in equilibrium with liquid water at 273.3 K and compared with a frost point hygrometer. These water vapor measurements are described below.

(i) Lyman- α absorption measurement. Determining the H_2O concentration via absorption of Lyman- α radiation utilized a 1, 19 or 50 cm long glass absorption cell equipped with MgF_2 windows and located upstream of the reactor where $O(^3P)$ temporal profiles were measured. Lyman- α light was produced by a microwave discharge lamp through which UHP He doped with a small amount of H_2 was rapidly flowed. The 121.6 nm line from the lamp was isolated from other lines (that are inevitably present in a microwave discharge) by a 0.3 m vacuum UV monochromator and detected by a solar blind PMT (110–200 nm). The output of the PMT was sampled at 10 Hz. The VUV light emanating from the opposite end of the discharge lamp was filtered through a glass cell containing O_2 and detected with a second PMT to correct, if necessary, for small drifts in the overall intensity of the lamp. $O(^3P)$ temporal profiles were measured with and without H_2O in rapid succession to further account for any drifts in lamp intensity or water vapor concentration.

(ii) Determination of the absorption cross section of H_2O at 121.6 nm. A 1 cm absorption cell with a cold finger containing liquid water held at 273.3 K in an ice/water bath was used to provide water vapor in equilibrium with liquid H_2O . The resulting absorption of 121.6 nm light was measured to obtain H_2O absorption cross section at this wavelength. Uncertainty in the vapor pressure of water was estimated to be $\pm 3\%$ based

on the uncertainty in the measured bath temperature. The average absorption cross section for water vapor at 121.6 nm, determined from eight such measurements, was $(1.5 \pm 0.2) \times 10^{-17} \text{ cm}^2$, in good agreement with the published literature value^{13,14} of $(1.59 \pm 0.10) \times 10^{-17} \text{ cm}^2$ (quoted uncertainties are at the 2σ level).

(iii) Determination of the absorption cross section of H₂O at 184.9 nm. The absorption cross section of water vapor at 184.9 nm was measured in a 100 cm glass cell that was connected in tandem to a 19 cm cell. A Hg pen lamp, a 185 nm band pass filter, and a phototube detector (160–200 nm) were used to generate, isolate, and measure the 184.9 nm radiation. The 100 cm cell was used for 184.9 nm absorption measurements, while the 19 cm cell was used for 121.6 nm. In addition to measuring water vapor concentration *via* light absorption, the pressure of pure water vapor that was either flowed through the absorption cell or filled statically into the cell, was measured by a 10 Torr capacitance manometer; absorption of 184.9 nm radiation at various pressures was measured. Lastly, water vapor in equilibrium with liquid water (as described earlier) was also used. The measured absorbances at 184.9 nm are plotted in Fig. 2 against water vapor concentrations determined by these three methods. From this data, we obtain an absorption cross section of H₂O at 184.9 nm of $(7.1 \pm 0.1) \times 10^{-20} \text{ cm}^2$ (2σ uncertainty); this value is in excellent agreement with $(7.14 \pm 0.20) \times 10^{-20} \text{ cm}^2$ previously determined by Cantrell *et al.*¹⁵ Our results confirm the results of Cantrell *et al.*, which were $\sim 30\%$ larger than the previously recommended value.¹⁶

(iv) Comparison of water vapor concentration measured using Lyman- α absorption and frost point hygrometer. Frost point hygrometers (FPH) are commonly used for measuring water vapor abundance in the atmosphere.^{17,18} A FPH was placed in series with a 19 cm absorption cell where the 121.6 nm absorption was measured. Dilute mixtures of H₂O in He were flowed through both the FPH and the absorption cell. The H₂O concentration was varied between $(1-9) \times 10^{14} \text{ molecule cm}^{-3}$. The average ratio of the H₂O concentration as measured by absorption at 121.6 nm to that measured by the FPH was 0.94 ± 0.45 (at the 95% confidence level). (After the sixth intercomparison point, a thermistor on the FPH burned out, inhibiting further measurements.)

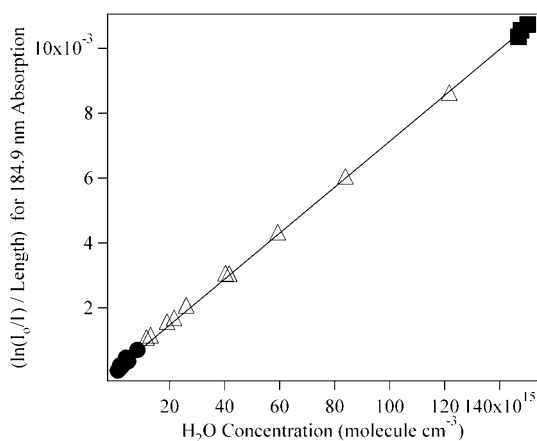


Fig. 2 A plot of the absorbance at 185 nm divided by the path length *versus* the known concentration of water vapor. The H₂O concentration was determined in three separate ways: by the Lyman- α absorption measurement (solid circles), by the measurement of the water vapor pressure with a capacitance manometer (open triangles), and by the known saturated water vapor pressure in equilibrium with liquid H₂O (solid squares). The slope of this plot gives the absorption cross section for H₂O at 185 nm = $(7.1 \pm 0.1) \times 10^{-20} \text{ cm}^2$.

Agreement amongst the four methods shows that we could accurately measure H₂O concentrations. Based on these measurements, the overall uncertainty in the water vapor concentration measurement at the 95% confidence level was estimated to be $\pm 5\%$ and $\pm 8\%$ for the Lyman- α and 185 nm absorption techniques, respectively. These uncertainties are reflected in the reported values of the rate coefficients.

Results

Absolute rate coefficient measurements

Temporal profiles of O(³P) (described in the experiment section) were recorded in the presence of various concentrations of H₂O while keeping the O₃ and He concentrations constant (see Table 1) and are described by the equation:

$$[\text{O}(\text{}^3\text{P})]_t = Ae^{-Bt} + Ce^{-Dt} \quad (\text{II})$$

where the parameters *A–D* are:

$$A = [\text{O}(\text{}^1\text{D})]_0 \frac{k_5[\text{O}_3] + k_1[\text{H}_2\text{O}]}{(D - B)} \quad (\text{III})$$

$$B = k_5[\text{O}_3] + k_1[\text{H}_2\text{O}] + k_7 \quad (\text{IV})$$

$$C = [\text{O}(\text{}^3\text{P})]_0 - A \quad (\text{V})$$

$$D = k_6 \quad (\text{VI})$$

In the above equations, *k*₆ is the first order rate coefficient for the loss of O(³P) from the detection region (defined by the overlap between the photolysis laser beam and probe beam from the microwave discharge lamp⁹) and *k*₇ is the first order rate coefficient for the removal of O(¹D) due to reaction with impurities in the bath gas. The first order rate coefficient for the rise (formation) of O(³P), the *B* parameter in eqn. (III), equals the overall first order rate coefficient for the loss of O(¹D), which is referred to as *k*. The temporal profiles were fit to expression (I) by using a non-linear least squares routine. The value of *D* was fixed in the fit by measuring it at longer reaction times. The details of the analysis and expected uncertainties in the obtained values of *k*' are given elsewhere.⁶ Briefly, the measured temporal profiles were fit to eqn. (I) such that the same percentage weight was given to the decaying part of the profile in all profiles. This approach, *i.e.*, using a measured value of *D* and the same fractional weight for the decay component, yielded very consistent fits with residuals that had no correlation with the rising or falling parts of the profile. Further, they properly weighted the rise, which determines the value of *B*. It was estimated that the uncertainty in *B* due to the fitting routine was roughly 3% or better.⁶

In order to compare various temporal profiles recorded with different O₃ concentrations, a value for *B* recorded without H₂O present was subtracted from each value of *B* measured in the presence of H₂O; this resulting value is referred to as *k*₁'. A plot of the measured values of *k*₁' *versus* the H₂O concentration at 295 K is shown in Fig. 3. The weighted linear least squares fit is shown, where the uncertainties in both *k*₁' and [H₂O] have been propagated. The intercept of this plot is not statistically different from zero, as it should be from our definition of *k*₁'. The slope of this plot is *k*₁. *k*₁ was measured at nine temperatures between 235 to 370 K. The obtained results are presented in Fig. 4 in the Arrhenius form. Table 1 lists the measured values at each temperature along with the experimental conditions used. The results for the absolute measurements of *k*₂ and *k*₃ have been presented in other studies.^{3,6}

Relative rate experiments

The values of *k*₁ relative to *k*₂ and relative to *k*₃ were determined by measuring the absolute values of OH

Table 1 The measured values of k_1 along with the experimental conditions used to determine the rate coefficients. The quoted uncertainties in k_1 are 2σ precision obtained by the linear least squares analyses of k' versus $[\text{H}_2\text{O}]$ data

T/K	P/Torr	Flow velocity/ cm s^{-1a}	$[\text{O}_3]/10^{13} \text{ cm}^{-3}$	Fluence/ $\text{mJ pulse}^{-1} \text{ cm}^{-2b}$	$[\text{O}(^1\text{D})]_0/10^{11} \text{ cm}^{-3}$	$[\text{H}_2\text{O}]/10^{13} \text{ cm}^{-3}$	k'/s^{-1}	$k_1/10^{-10}$ $\text{cm}^{-3} \text{ s}^{-1}$
235	34	10.6	2.33	1.6	7.5	2.37–6.31	8000–25 900	2.00 ± 0.26
240	22	17.9	1.20	3.0	8.0	1.30–8.30	5400–28 650	2.35 ± 0.24
240	23	16.3	1.10	3.5	8.0	1.19–6.42	4200–18 320	2.17 ± 0.14
240	23	16.6	1.32	1.4	4.0	1.97–6.53	6400–19 900	1.81 ± 0.17
240						weighted average		2.07 ± 0.23
250	26	14.7	1.60	2.3	7.7	0.88–7.30	6300–25 000	2.18 ± 0.13
260	28	14.7	1.00	3.2	7.5	0.80–7.68	5200–22 540	2.14 ± 0.32
260	35	11.4	2.18	1.8	8.2	0.94–5.59	7300–17 200	2.52 ± 0.26
260	22	18.9	1.18	1.8	5.0	1.68–9.84	5900–25 500	2.07 ± 0.24
260						weighted average		2.25 ± 0.16
280	23	19.1	1.20	1.8	5.0	1.94–8.89	5500–23 300	1.96 ± 0.09
295	34	13.8	1.10	3.1	7.5	1.60–8.30	5400–22 540	2.00 ± 0.40
295	33	13.8	0.87	3.3	7.0	1.36–7.50	6500–27 250	2.30 ± 0.24
295	36	12.6	0.94	3.3	6.6	1.70–5.90	5400–17 950	2.14 ± 0.31
295	30	15.4	1.04	2.8	5.4	2.37–8.45	4300–20 200	1.81 ± 0.07
295	30	15.2	1.78	1.3	5.7	1.10–8.40	6200–20 100	2.03 ± 0.06
295	20	22.5	1.08	2.0	5.1	2.97–7.25	5500–19 800	1.97 ± 0.19
295						weighted average		1.96 ± 0.08
330	36	14.1	1.10	3.3	6.0	1.50–6.88	5100–17 750	1.86 ± 0.12
330	23	22.3	0.99	2.0	4.0	1.22–6.61	5000–17 300	1.84 ± 0.15
332	34	14.9	1.48	2.8	9.1	2.49–7.50	5300–20 200	1.71 ± 0.09
331						weighted average		1.78 ± 0.08
350	23	23.9	0.90	2.0	3.0	1.56–7.73	4900–19 000	1.87 ± 0.13
370	38	14.9	1.38	3.3	9.0	1.30–7.27	5350–19 680	1.90 ± 0.17
370	30	19.1	1.55	1.5	5.0	0.60–8.10	5500–25 000	2.13 ± 0.13
370	26	21.2	1.25	2.0	6.0	1.22–6.27	5400–16 500	1.76 ± 0.13
370						weighted average		1.93 ± 0.10

^a Linear flow velocity measured in the center of the reaction cell. ^b All experiments run at a repetition rate of 4 Hz.

concentrations produced from Reaction (1) at various concentrations of N_2 or O_2 while maintaining a fixed H_2O concentration. To account for changes in detection sensitivity with varying concentrations of N_2 and O_2 , we “calibrated” the OH detection system by measuring the OH signal from the photolysis of a measured concentration of H_2O_2 added to this mixture, *i.e.*, under conditions identical to those used for measuring relative signal levels in N_2 and O_2 . These experiments were done in sets of back-to-back measurements; in the first run, a mixture of $\text{He}/\text{H}_2\text{O}/\text{H}_2\text{O}_2$ was photolyzed at 248 nm to produce OH; in the second run,

O_3 was added to the same mix as in the first run and photolyzed with the same fluence, so as to produce additional OH from Reaction (1). For clarity, the subscript “ H_2O_2 ” refers to the first half of the back-to-back pair with just H_2O_2 present and the subscript “ O_3 ” refers to the second half with H_2O_2 and O_3 present.

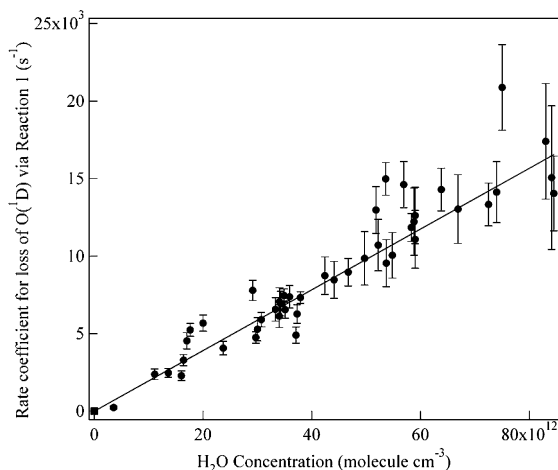


Fig. 3 A plot of the first order rate coefficient for loss of $\text{O}(^1\text{D})$ versus concentration of H_2O at 295 K. The slope is the bimolecular rate coefficient for total removal of $\text{O}(^1\text{D})$ by the reactant via both reaction and quenching. A linear weighted fit gives a slope of $(1.96 \pm 0.18) \times 10^{-10}$ and an intercept of -14 ± 50 (2σ uncertainties).

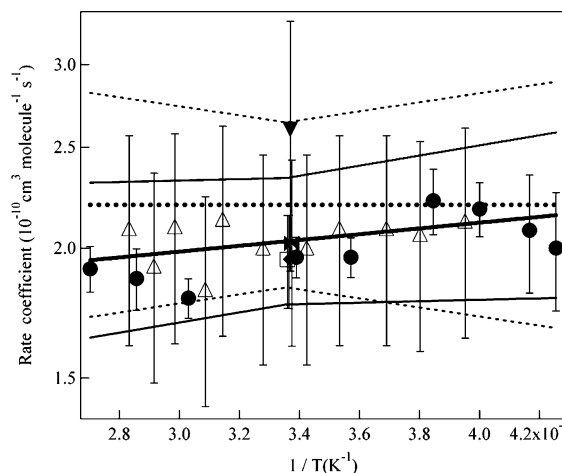


Fig. 4 Arrhenius plot for Reaction (1) showing k_1 (on a logarithmic scale) against the inverse of the temperature. Previous temperature dependent studies from Table 3 are shown along with the results from this study and the new recommendation. Streit *et al.*, 1976 = open triangles; Amimoto *et al.*, 1979 = solid diamond; Lee and Slinger, 1979 = solid triangle; Wine and Ravishankara, 1981 = open square; Gericke and Comes, 1981 = solid bow tie; This work = solid circles; JPL, 2000 = thick dashed line (95% confidence limits = thin dashed lines); Our recommendation = thick solid line (95% confidence limits = thin solid lines).

In the presence of He/H₂O/H₂O₂, the OH temporal profiles were exponential and the time constants for the decay of OH was controlled by its reaction with H₂O₂. These temporal profiles were extrapolated to time zero to obtain signal ($S_{\text{H}_2\text{O}_2}$) attributed to the OH concentration produced from H₂O₂ photolysis:

$$[\text{OH}]_{\text{H}_2\text{O}_2} = F_{\text{H}_2\text{O}_2} \times \sigma_{\text{H}_2\text{O}_2} \times [\text{H}_2\text{O}_2] \times \Phi_{\text{H}_2\text{O}_2} \quad (\text{VII})$$

In the above equation, $F_{\text{H}_2\text{O}_2}$ is the 248 nm laser fluence, $\sigma_{\text{H}_2\text{O}_2}$ is the absorption cross section of H₂O₂ at 248 nm ($\sigma_{248}(\text{H}_2\text{O}_2) = 9.06 \times 10^{-20} \text{ cm}^2$),² $[\text{H}_2\text{O}_2]$ is the measured H₂O₂ concentration, and $\Phi_{\text{H}_2\text{O}_2}$ is the quantum yield for OH production from H₂O₂ photolysis² ($\Phi_{\text{H}_2\text{O}_2} = 2$). The absorption cross section and quantum yield have a combined uncertainty of $\pm 30\%$ at the 1σ level.²

In the presence of He/H₂O/H₂O₂/O₃, the initial OH signal (obtained from extrapolating the measured temporal profiles of OH to time zero) was due to OH from both H₂O₂ photolysis and O(¹D) reaction with H₂O. O(¹D) was produced from O₃ photolysis. The concentration of O(¹D) produced by the 248 nm laser is:

$$[\text{O}(\text{}^1\text{D})]_{\text{O}_3} = F_{\text{O}_3} \times \sigma_{\text{O}_3} \times [\text{O}_3] \times \Phi_{\text{O}_3} \quad (\text{VIII})$$

with $\sigma_{\text{O}_3} = 1.08 \times 10^{-17} \text{ cm}^2$, and $\Phi_{\text{O}_3} = 0.9$ at 248 nm. The absorption cross section and the quantum yield are from ref. 2. More than $1 \times 10^{16} \text{ molecule cm}^{-3}$ of water vapor was used such that the production of OH was almost exclusively from Reaction 1 and was instantaneous on the time scale of the measured temporal profile. Within 10 μs , the earliest time at which OH was detected, less than ten parts in a billion of O(¹D) was left over and greater than 90% of vibrationally excited OH was quenched to OH($\nu'' = 0$). The quenching of O(¹D) by He ($k(\text{O}(\text{}^1\text{D}) + \text{He}) < 10^{-15} \text{ cm}^3 \text{ molecule}^{-1} \text{ s}^{-1}$)^{6,19} was too slow to significantly compete with the reaction of O(¹D) with H₂O. The temporal profiles of OH were single exponential decays. The intercept in this exponential decaying profile, obtained *via* least squares analyses, was proportional to the sum of the OH produced from H₂O₂ photolysis and from the reaction of O(¹D) with H₂O; it is referred to as S_{O_3} . The amount of OH produced from Reaction (1) was thus proportional to ($S_{\text{O}_3} - S_{\text{H}_2\text{O}_2}$).

Water vapor is an efficient quencher of OH ($A^2\Sigma$). To account for the decrease in the observed laser induced fluorescence signal due to the quenching of OH($A^2\Sigma$) by H₂O, we normalized our signal by dividing the measured signal due to Reaction (1) by the signal from the H₂O₂ photolysis with the same concentration of H₂O:

$$S' = \frac{(S_{\text{O}_3} - S_{\text{H}_2\text{O}_2})}{S_{\text{H}_2\text{O}_2}} \quad (\text{IX})$$

The signal level also fluctuated slightly due to variations in the probe laser fluence and small drifts in the probe wavelength. This normalized signal was also corrected for small (measured) variations in the probe and photolysis laser fluences and variations in the concentrations of H₂O₂ and O₃. To recognize and to minimize drifts in energies and concentrations, we measured $S_{\text{H}_2\text{O}_2}$, then S_{O_3} , and then $S_{\text{H}_2\text{O}_2}$ again. We rejected data where the signal levels in these “back-to-back-to-back” experiments changed significantly; such changes, however, were very infrequent.

We determined the relative values of k_1/k_2 or k_1/k_3 by measuring the normalized signal, S' , from O(¹D) reacting with a certain amount of H₂O, then adding various amounts of N₂ or O₂ to reduce the amount of O(¹D) available for reaction with H₂O. Using N₂ as the example, the signal due to OH from Reaction (1) in the absence of N₂, S'_0 , is related to the OH signal in the presence of N₂, S' , by the relation:

$$S' = S'_0 \times \frac{k_1[\text{H}_2\text{O}]}{k_1[\text{H}_2\text{O}] + k_2[\text{N}_2]} \quad (\text{X})$$

or:

$$\frac{1}{S'} = \frac{1}{S'_0} \times \frac{k_1[\text{N}_2]}{k_1[\text{H}_2\text{O}]} + \frac{1}{S'_0} \quad (\text{XI})$$

A plot of $1/S'$ versus $[\text{N}_2]/[\text{H}_2\text{O}]$ has a slope of $1/S'_0 \times (k_2/k_1)$ and an intercept of $1/S'_0$. The ratio, k_2/k_1 , is equal to the slope divided by the intercept. Plots of $1/S'$ versus $[\text{N}_2]/[\text{H}_2\text{O}]$ and $[\text{O}_2]/[\text{H}_2\text{O}]$ are shown in Fig. 5a and b respectively. Table 2 lists the experimental conditions for these measurements. From these measured values, we obtain the ratios $k_2/k_1 = 0.131 \pm 0.041$ and $k_3/k_1 = 0.193 \pm 0.090$. Uncertainties in the slope, the intercept, and the systematic uncertainty from the reactant concentration measurements were added together in quadrature to derive the overall uncertainty in the relative rate coefficients reported above.

Yield of OH from the reaction O(¹D) + H₂O

Using the same experimental set up as that used for the relative rate coefficient studies described above, we also determined the yield of OH from the reaction of O(¹D) with H₂O. Similar back-to-back experiments as in those described above were performed, but in the absence of N₂ or O₂. The yield of OH per O(¹D) atom was calculated from the following, using the same definitions as above for the “H₂O₂” and “O₃” runs in

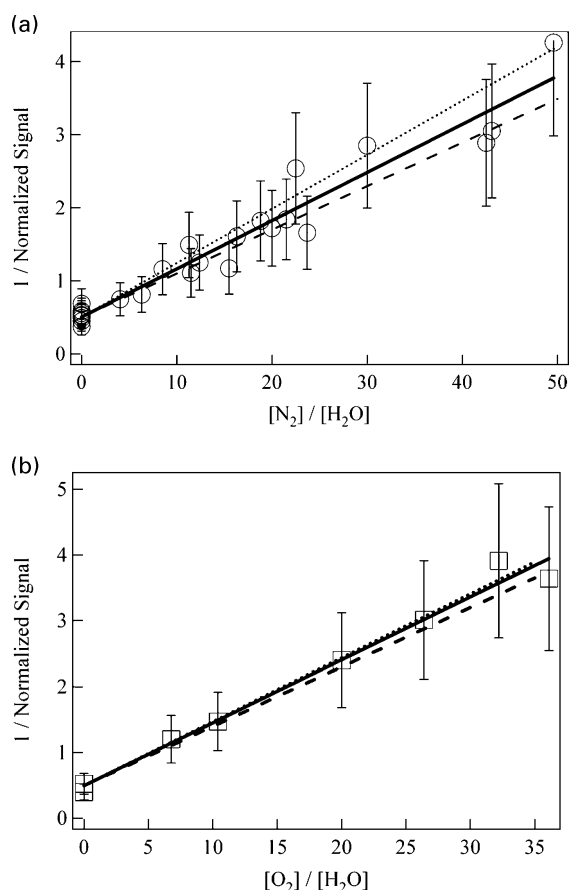


Fig. 5 (a) A plot of the inverse of the normalized OH signal versus the ratio of the N₂ concentration to the H₂O concentration. Solid line is a linear least squares fit to the data (open circles); long dashed line is from JPL, 2000 rate coefficients; short dashed line is from our measured values of the rate coefficients. (b) A plot of the inverse of the normalized OH signal versus the ratio of the O₂ concentration to the H₂O concentration. Solid line is a linear least squares fit to the data (open squares); long dashed line is from JPL, 2000 rate coefficients; short dashed line is from our measured values of the rate coefficients.

Table 2 Experimental conditions used for relative rate coefficient measurements

Compound	N ₂	O ₂
Total pressure (Torr)	50	50
Total flow rate (sccm)	(400–450)	450
[H ₂ O] ^a	(3–4) × 10 ¹⁴	(3–4) × 10 ¹⁴
[O ₃] ^a	(1.5–2) × 10 ¹³	2 × 10 ¹³
Fluence (mJ pulse ⁻¹)	2.8–8.0	3.7–16.0
[OH] from H ₂ O ₂ photolysis ^a	(2–6) × 10 ¹¹	(5–15) × 10 ¹¹
[O(¹ D)] from O ₃ photolysis ^a	(6–25) × 10 ¹¹	(10–50) × 10 ¹¹
[H ₂ O] ^a	(3–6) × 10 ¹⁶	(4–6) × 10 ¹⁶
[N ₂] or [O ₂] ^a	(0–1.5) × 10 ¹⁸	(0–1.6) × 10 ¹⁸
Slope of fit to data	0.51 ± 0.14	0.50 ± 0.22
Intercept of fit to data	0.066 ± 0.007	0.096 ± 0.010

^a All concentrations in the units of molecule cm⁻³.

the back-to-back pair:

$$\text{OH Yield} = \frac{S_{\text{O}_3} - S_{\text{H}_2\text{O}_2}}{S_{\text{H}_2\text{O}_2}} \times \frac{[\text{OH}]_{\text{H}_2\text{O}_2}}{[\text{O}(\text{}^1\text{D})]_{\text{O}_3}} \quad (\text{XI})$$

Additionally, we accounted for small variations in the H₂O₂ concentration or laser fluence between runs within the back-to-back pair.

We measured the yield of OH from Reaction (1) at room temperature at a total pressure of 50 Torr, with (3–18) × 10¹⁶ molecule cm⁻³ of H₂O, (9–94) × 10¹⁰ molecule cm⁻³ of OH produced from H₂O₂ photolysis and (20–300) × 10¹⁰ molecule cm⁻³ of O(¹D) produced from O₃ photolysis. The average value of 41 individual measurements of the OH yield was 1.93^{+0.07}/_{-0.45}. The uncertainty is twice the standard deviation of the individual yield measurements; systematic uncertainties were negligible in comparison.

Discussion

Rate coefficient for O(¹D) + H₂O reaction

Our result for k_1 at room temperature agrees, given the combined uncertainties, with the current recommendation of k_1 (298 K) = 2.2 × 10⁻¹⁰ cm³ molecule⁻¹ s⁻¹,² which is the average of the five previous determinations listed in Table 3. As can be seen in the table, the value of Lee and Slanger²⁰ is the farthest away from ours. Our result agrees well with the other four previous values reported in the table. Lee and Slanger measured k_1 primarily to ascertain which of the two reported values at that time, the results of Streit *et al.*²¹ and of Heidner and Husain,²² was accurate. They measured k_1 at 298 K by following the temporal profile of O(¹D) in the presence of different concentrations of H₂O. The rate coefficient reported by them was obtained from a visual best fit of their data. We digitized their measured values of the first order rate coefficients

for O(¹D) loss as a function of water vapor concentration reported in their Fig. 1. A linear least squares analysis of that data yields $k_1 = (2.65 \pm 0.70) \times 10^{-10}$ cm³ molecule⁻¹ s⁻¹, with an intercept that is essentially zero (-137 ± 2070 s⁻¹). Here the quoted error bars for the slope and the intercept are the two sigma uncertainties obtained solely from the linear regression. This value compares quite well with that derived by the authors, $(2.6 \pm 0.5) \times 10^{-10}$ cm³ molecule⁻¹ s⁻¹, but suggests that they underestimated their uncertainty somewhat. Lee and Slanger did not directly measure the concentration of H₂O in the gas mixture in the reactor, but derived it from the known vapor pressure of H₂O in a bubbler through which the diluent gas was flowed. They asserted that their measured rate coefficient would be a lower limit because they believed that the water vapor concentration in the reactor was, if anything, lower than what they had derived because water could be lost on the walls of the reactor and the gas flow system. However, this is not necessarily always the case, and one could get desorption from the walls and thus enhance the water vapor concentration. If we were to take the previously reported values and assume that the errors are purely statistical, we could exclude Lee and Slanger's data based on Chauvernet's criterion.²³ However, it is unlikely that the errors are only statistical. In any case, it is clear that Lee and Slanger's data overlaps with the average value recommended here within the error bounds derived from their plot. Again, it is worth reiterating that the measurements of Lee and Slanger were for the specific purpose of distinguishing between the disparate results that were available at that time and it clearly showed that the results of Streit *et al.* were more accurate.

Because of the above reasons, we have excluded the results of Lee and Slanger's in deriving our recommended value for atmospheric calculations of k_1 (298 K) = (2.0 ± 0.2) × 10⁻¹⁰ cm³ molecule⁻¹ s⁻¹; this value is based on the average of our result with the other four studies listed in Table 3. As with many other reactions of O(¹D), we have not included the results of Heidner and Hussain. We note that the largest source of uncertainty in measuring k_1 will be the determination of the concentration of water vapor and that our study used an *in situ* measurement of the H₂O concentration, which was compared with three other separate methods, such that we have greatly reduced this uncertainty.

We measured a small negative temperature dependence for k_1 , $E_a/R = (-80 \pm 90)$ K. The only previous determination of the temperature dependence of k_1 was that by Streit *et al.*²¹ They did not report the uncertainties associated with each determination of k_1 as a function of temperature. They asserted that their rate coefficient did not change with temperature based on a visual inspection. If we were to fit their data to an Arrhenius expression ($\ln k_1 = \ln A - E_a/RT$) using a linear least squares analysis, we obtain $k_1 = (2.05 \pm 0.40) \times 10^{-10} \exp \{(-35 \pm 57)/T\}$ cm³ molecule⁻¹ s⁻¹. Here the $\sigma_A = A \sigma_{\ln A}$ and the quoted uncertainties are twice the standard deviations obtained by the least squares fit.

Table 3 Comparison of our measured values of k_1 with those in the literature

Temperature range/K	298 K rate coefficient ^a	Arrhenius A factor ^a	Arrhenius (E_a/R)/K	f (298 K)	Reference
253–353	2.3 ± 0.5 1.95 ± 0.3 2.6 ± 0.5 1.95 ± 0.2 2.02 ± 0.41	2.3 ± 0.5	0		Davidson (Streit) <i>et al.</i> , 1976 ²¹ Amimoto <i>et al.</i> , 1979 ³³ Lee and Slanger, 1979 ²⁰ Wine and Ravishankara, 1981 ⁸ Gericke and Comes, 1981 ³⁴
253–353	2.2 ± 0.44	2.2 ± 0.44	0 ± 100	1.2	JPL, 2000 ²
235–370	1.96 ± 0.18	1.45 ± 0.34	-89 ± 65		This work
235–370	2.03 ± 0.28	1.62 ± 0.27	-65 ± 50	1.15	Recommendation

^a Units of × 10⁻¹⁰ cm³ molecule⁻¹ s⁻¹.

Combining our results with those from Streit *et al.* and refitting all of the data together, we determine an E_a/R value of (-65 ± 50) K. A small negative activation energy for Reaction (1) is consistent with the expected absence of a barrier for $O(^1D)$ insertion into H_2O and the large value of k_1 .

Relative rate coefficient measurements

One potential complication in our experiments on measuring the ratios of the rate coefficients k_1/k_2 and k_1/k_3 was the possible production of OH from the photolysis of H_2O at 248 nm. The absorption cross section for H_2O at 248 nm is small enough ($\ll 10^{-21} \text{ cm}^2$) to rule out significant OH production *via* single photon absorption at the concentrations of H_2O used in our experiments. We tested for OH production from multi photon photolysis by irradiating a large concentration of H_2O ($1 \times 10^{17} \text{ molecule cm}^{-3}$) with a large fluence of 248 nm laser light ($20 \text{ mJ pulse}^{-1} \text{ cm}^{-2}$); such large concentrations and fluences were not used in measuring the ratio of rate constants. In this test, no OH signal was observed and an upper limit of $[OH] < 7 \times 10^9 \text{ molecule cm}^{-3}$ was determined. This concentration was $< 4\%$ of the smallest initial OH concentration generated during any subsequent measurements (after accounting for differences in LIF quenching signal), so we conclude that production of OH by direct photolysis of H_2O was negligible for our experiments.

In general, the values of k_1/k_2 and k_1/k_3 measured here agree with that calculated from the individual values of k_1 – k_3 measured recently in our laboratory, given the uncertainties in the relative measurements. Our measured value of k_2/k_1 is 11% higher than the ratio calculated from the previously recommended rate coefficients² (0.118) and 15% lower than the ratio calculated from our directly measured values (0.154). However, they all agree within the quoted uncertainty limits. Our measurement of k_3/k_1 is only 6% higher than the ratio calculated from the previous recommendations² (0.182) and is in excellent agreement with the ratio calculated from our direct measurements of the individual rate coefficients (0.196). Thus we believe that the individual values of k_1 – k_3 are determined with an accuracy better than 15%.

Yield of OH from the reaction $O(^1D) + H_2O$

As stated (see introduction), Reaction (1) has several exothermic channels available at room temperature. Reaction channel (1a) has been shown previously to be the dominant channel.² The yield of Reaction 1b, Φ_{1b} , has been measured by Wine and Ravishankara²⁴ to be $\Phi_{1b} = (4.9 \pm 3.2)\%$, and by Takahashi *et al.*²⁵ to be $\Phi_{1b} = (2 \pm 1)\%$. Zellner *et al.*²⁶ measured a yield for Reaction (1c), $\Phi_{1c} = (1^{+0.5}/_{-1})\%$, and Glinski and Birks²⁷ measured $\Phi_{1c} = (0.6^{+0.7}/_{-0.6})\%$. Our measurement of the OH yield of $1.93^{+0.07}/_{-0.45}$ agrees well with these previous studies and is consistent with OH being the dominant product of Reaction (1).

Atmospheric implications

We can now revisit the calculation of the uncertainty in the atmospheric OH production rate. Extrapolating the uncertainties in our recommended individual rate coefficients, k_1 – k_3 , leads to a total uncertainty in the atmospheric OH production rate due to the rate coefficients of $\pm 15\%$. The relative rate coefficient studies provide further confirmation of this conclusion.

In order to evaluate the consequences of the rate coefficients and rate coefficients ratios measured here to the calculated atmospheric OH production rates, we have employed a simple box model based on the US Standard Atmosphere²⁸ for the atmospheric profiles of temperature, pressure, N_2 , O_2 , H_2O (mid latitude mean from the Standard Atmosphere), CO_2 (360 ppmv), O_3 (350 Dobson Units), H_2 ,²⁹ N_2O ,³⁰ CO ,³⁰

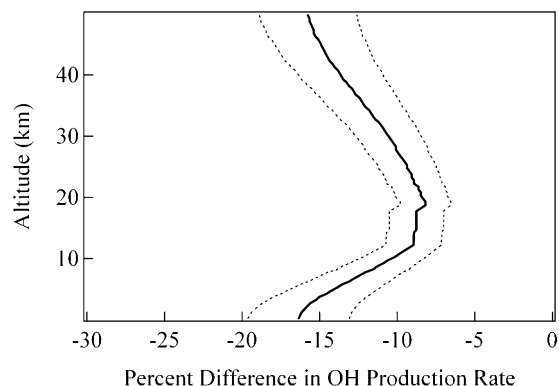


Fig. 6 Percentage change in the atmospheric OH production rate in switching from the JPL 2000 recommended $O(^1D)$ rate coefficients to our recommended values plotted *versus* altitude (solid line) along with the 2σ uncertainty in that change (dashed lines).

and CH_4 .³⁰ The J -values for $O(^1D)$ production were determined using the Tropospheric Ultraviolet-Visible Radiation model developed at NCAR³¹ (summed from 200–400 nm with 1 nm wide bins centered on the integer wavelengths). The extraterrestrial flux from the Susium/Neckel satellite³¹ for northern hemisphere spring equinox was used. No aerosols were incorporated, and the albedo was set at 5%. The $O(^1D)$ quantum yields from O_3 photolysis were from Talukdar *et al.*³² We solved for the steady state concentrations of $O(^1D)$ and OH and the OH production rate as a function of altitude.

The fractional (percentage) change in the calculated OH production rates using our rate coefficients relative to that calculated from the recommended values is displayed in Fig. 6. The calculated OH production rate decreased by as much as 15% due to our rate coefficient measurements. More importantly, Fig. 6 also shows that the uncertainty in the calculated OH production rate is approximately 20%. These uncertainties were calculated by setting the values of k_1 – k_3 to their maximum possible ranges (*i.e.*, $k + 2\sigma$ and $k - 2\sigma$) derived from this study. Given these results, we conclude that the overall uncertainty in the OH production rate due to the uncertainty in the rate coefficients involved has been narrowed to less than $\pm 20\%$. This estimate is consistent with the uncertainty derived from the measured ratios of rate coefficients, *i.e.*, k_1/k_2 and k_1/k_3 , and is slightly larger than the uncertainty derived from the individually measured rate coefficients so as to provide a conservative conclusion.

Acknowledgements

This work was funded in part by NASA's Upper Atmosphere Research Project and NASA's Earth System Science doctoral Fellowship to EJD.

References

- 1 B. J. Finlayson-Pitts and J. N. Pitts, *Atmospheric Chemistry: Fundamentals and Experimental Techniques*, John Wiley & Sons Inc., New York, 1986.
- 2 S. P. Sander, D. M. Golden, R. F. Hampson, M. J. Kurylo, C. J. Howard, A. R. Ravishankara, C. E. Kolb and M. J. Molina, *Chemical kinetics and photochemical data for use in stratospheric modeling*, Jet Propulsion Laboratory, California Institute of Technology Evaluation, 2000, No. 13, JPL Publication 00-3.
- 3 A. R. Ravishankara, E. J. Dunlea, M. A. Blitz, T. J. Dillon, D. E. Heard, M. J. Pilling, R. S. Strekowski, J. M. Nicovich and P. H. Wine, *Geophys. Res. Lett.*, 2002, **29**, 10.1029/2002GL014850.
- 4 R. S. Strekowski, J. M. Nicovich and P. H. Wine, *Phys. Chem. Chem. Phys.*, 2004, **6**, 10.1039/b400243a.
- 5 D. Heard, M. A. Blitz, T. J. Dillon, M. Pilling and I. D. Trought, *Phys. Chem. Chem. Phys.*, 2004, **6**, 10.1039/b400283k.

- 6 E. J. Dunlea and A. R. Ravishankara, *Phys. Chem. Chem. Phys.*, 2004, **6**, 10.1039/b400247d.
- 7 R. F. Warren and A. R. Ravishankara, *Int. J. Chem. Kinet.*, 1993, **25**, 833–844.
- 8 P. H. Wine and A. R. Ravishankara, *Chem. Phys. Lett.*, 1981, **77**, 103–109.
- 9 E. J. Dunlea, Ph.D. Thesis, *Department of Chemistry and Biochemistry*, University of Colorado, Boulder, 2002.
- 10 A. A. Turnipseed, G. L. Vaghjiani, J. E. Thompson and A. R. Ravishankara, *J. Chem. Phys.*, 1992, **96**, 5887–5895.
- 11 G. L. Vaghjiani and A. R. Ravishankara, *J. Phys. Chem.*, 1989, **93**, 1948–1959.
- 12 G. L. Vaghjiani and A. R. Ravishankara, *J. Chem. Phys.*, 1990, **92**, 996–1003.
- 13 D. Kley, *J. Atmos. Chem.*, 1984, **2**, 203–210.
- 14 R. K. Vatsa and H.-R. Volpp, *Chem. Phys. Lett.*, 2001, **340**, 289–295.
- 15 C. A. Cantrell, A. Zimmer and G. S. Tyndall, *Geophys. Res. Lett.*, 1997, **24**, 2195–2198.
- 16 R. D. Hudson, *Can. J. Chem.*, 1974, **52**, 1465–1478.
- 17 S. J. Oltmans, *Measurement and Control in Science and Industry, Proceedings of the 1985 International Symposium on Moisture and Humidity*, 1985, 251–258.
- 18 H. Vomel, S. J. Oltmans, D. J. Hofmann, T. Deshler and J. M. Rosen, *J. Geophys. Res.*, 1995, **100**, 13919–13926.
- 19 J. Shi and J. R. Barker, *Int. J. Chem. Kinet.*, 1990, **20**, 1283–1301.
- 20 L. C. Lee and T. G. Slanger, *Geophys. Res. Lett.*, 1979, **6**, 165–166.
- 21 G. E. Streit, C. J. Howard and A. L. Schmeltekopf, *J. Phys. Chem.*, 1976, **65**, 4761–4764.
- 22 R. F. I. Heidner, D. Husain and J. R. Wiesenfeld, *J. Chem. Soc., Faraday Trans. 2*, 1973, **69**, 927–938.
- 23 J. R. Taylor, *An Introduction to Error Analysis*, University Science Books, Mill Valley, California, 1982.
- 24 P. H. Wine and A. R. Ravishankara, *Chem. Phys.*, 1982, **69**, 365–373.
- 25 K. Takahashi, R. Wada, Y. Matsumi and M. Kawasaki, *J. Phys. Chem.*, 1996, **100**, 10 145–10 149.
- 26 R. Zellner, G. Wagner and B. Himme, *J. Phys. Chem.*, 1980, **84**, 3196–3198.
- 27 R. J. Glinski and J. W. Birks, *J. Phys. Chem.*, 1985, **89–90**, 3449–3453342.
- 28 U.S. Standard Atmosphere, U.S. Government Printing Office, U.S. Standard Atmosphere, 1976.
- 29 G. Brasseur and S. Solomon, *Aeronomy of the Middle Atmosphere*, 2nd edn., D. Reidel Publishing Company, Dordrecht, 1986.
- 30 R. Goody, *Principles of Atmospheric Physics and Chemistry*, Oxford University Press Inc., New York, 1996.
- 31 S. Madronich, J. Zeng and K. Stamnes, Tropospheric ultraviolet-visible radiation model, Version 3.8, 1997.
- 32 R. K. Talukdar, C. A. Longfellow, M. K. Gilles and A. R. Ravishankara, *Geophys. Res. Lett.*, 1998, **25**, 143–146.
- 33 S. T. Amimoto, A. P. Force, R. G. Gulotty, Jr. and J. R. Wiesenfeld, *J. Chem. Phys.*, 1979, **71**, 3640–3647.
- 34 K.-H. Gericke and F. J. Comes, *Chem. Phys. Lett.*, 1981, **81**, 218–222.